

IMPLEMENTATION OF ELECTRON-X-RAY BEAM OVERLAP DIAGNOSTIC INSTRUMENT AT LCLS

M. D. Balcazar*, A. Lutman, F. J. Decker, A. Montironi, D. Cesar, G. Franzen,
 H. Wang, X. Permanyer, D. Zhu, T. Sato, A. Halavanau, Z. Huang
 SLAC National Accelerator Laboratory, Menlo Park, CA, USA

Abstract

We report on the commissioning results of the newly implemented Beam Overlap Diagnostic (BOD) instrument at the hard X-ray line of the Linac Coherent Light Source (LCLS). As part of the CBXFEL project at SLAC, the instrument is designed to facilitate alignment between the relativistic electron beam entering the undulator line and the X-rays returning from the CBXFEL cavity via the return line. The station features two interchangeable targets: (1) a boron doped CVD diamond screen for direct imaging of the electron beam; and (2) a YAP:Ce scintillator for detecting returning X-rays in the cavity. Emission from either target, whether generated by electron-induced cathodoluminescence or X-ray-induced scintillation, is captured using a nanosecond-resolution fast-gated optical/UV camera. We present results from recent commissioning runs, including direct electron beam imaging, beam size and position characterization in both single- and two-bunch modes, and observations of coherent radiation linked to early microbunching, with implications for the laser heater configuration.

INTRODUCTION

For the next generation of X-ray free electron lasers (XFEL), the cavity-based XFEL is a promising approach to achieve fully coherent X-ray pulses and orders-of-magnitude increased brightness. At the Linac Coherent Light Source (LCLS) at SLAC, the Cavity-based X-ray Free Electron Laser (CBXFEL) project [1–6] aims to utilize four Bragg diamond crystals to circulate X-rays in a rectangular cavity scheme to seed a second electron bunch and achieve two-pass gain. One of the key requirements for the successful operation of the cavity is the ability to overlap the recirculating X-rays with the second fresh electron bunch. This overlap must be achieved both spatially and temporally in order to obtain lasing in the undulator. To achieve the spatial overlap between X-rays and electron beams, a specially designed instrument – known as Station F – was developed.

The paper presents the first commissioning results of Station F, including the direct observation of the LCLS relativistic electron beam in both single- and two-bunch modes. The size and position of the electron beam are directly measured using the beam overlap diagnostic (BOD) instrument across multiple shots. In addition, the effect of background radiation emission from optical microbunching instability along the electron accelerator is investigated, and its relationship to the laser heater energy is characterized.

EXPERIMENT

Setup

The experimental setup utilizes the hard X-ray beamline at LCLS. The BOD instrument, Station F, is located at the entrance of the undulator hall, right after the first CBXFEL chicane and before the first hard X-ray undulator (HXU). The electron bunch energy for this test was 10.7 GeV with a charge of 175.34 pC. Station F consists of two targets mounted on a paddle with a linear stage in the vertical direction. Each target can be individually selected by different encoder positions. The first target is a YAP:Ce with UV fluorescence, which is intended to capture returning X-rays in the cavity [6]. More relevant for this study is the second target, a 5 × 5 mm diamond screen which is suitable to directly image the electron beam through optical cathodoluminescence [7–10]. While the design for Station F consists of a gated Andor iStar camera with wide spectral acceptance, this initial experiment focused on exclusively imaging the electron beam, thus a simple GigE camera along with an optical lens were used. The exposure time was adjusted accordingly to capture the luminescence of the target after the interaction.

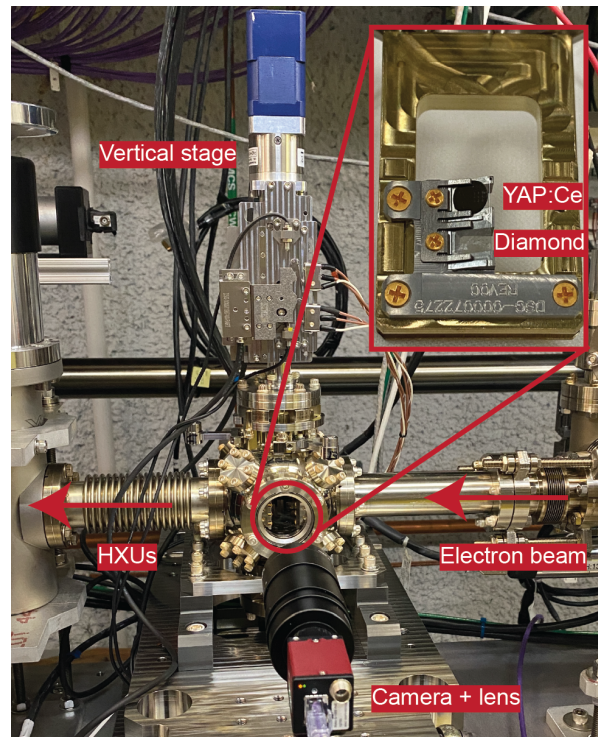


Figure 1: BOD instrument and its interchangeable targets.

* mdbm@slac.stanford.edu

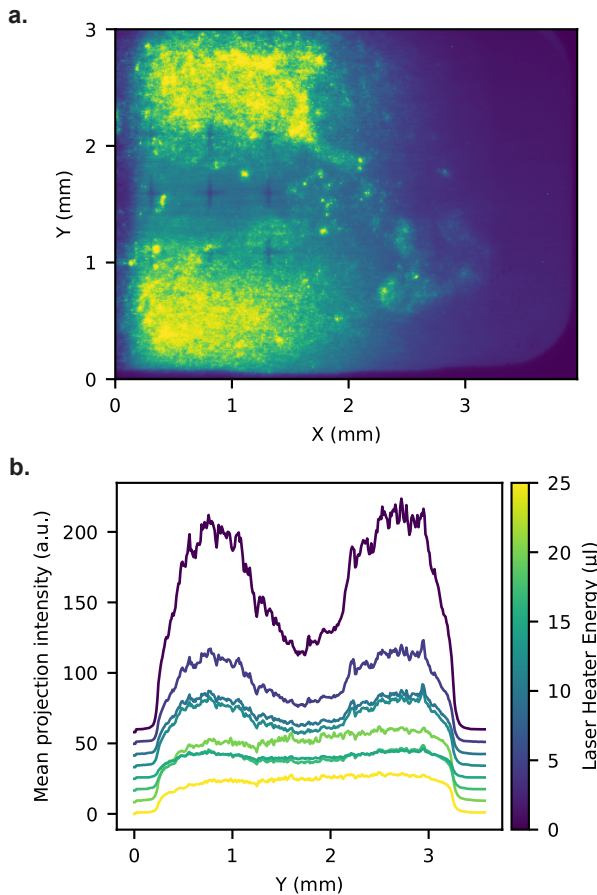


Figure 2: **a.** Background radiation pattern of the accelerator line recorded on diamond target. **b.** Integrated vertical line profiles of images taken over 60 pixel columns as a function of laser heater energy.

Experimental Results

An image of the diamond target is obtained by optical cathodoluminescence when excited by ultra-relativistic electrons. The luminescent light is redirected by an angled mirror into the camera through the lens. Before attempting to send the full electron beam into the diamond the chicane was first turned on at its full delay. The delay was initially set to a nominally large value, 300 fs, then reduced to smaller values: 250, 200, 150, 100, 50 fs. Large chicane delays results in the electron beam deflected laterally to the side of the diamond screen and not traversing through the target. The objective of this test was two-fold. First, for safety precautions, as the direct interaction of the relativistic electron beam and the diamond can result in secondary radiation generation potentially hazardous to the HXUs. Secondly, the background radiation profile on the diamond could be observed. An example of background radiation on the diamond target at ~100 fs is shown in Fig. 2a.

The result was a pattern consisting of two main lobes on top and bottom of the screen. We concluded that the main source of this background originated from the optical microbunching in the beam upstream on the undulator line. Laser heater is utilized to suppress this microbunching, as

shown in the lineouts of Fig. 2b. Thus, while Station F is designed to directly observe the electron beam this test proved that it has the potential to provide additional information. The background images were also used to calibrate the pixels to real physical values using a crossmark pattern etched on the target (crosses spaced $d = 0.5$ mm apart).

Naturally, the most important measurement of this study consisted of directly observing the position and size of the electron beam on the Station F diamond target. An effort to avoid saturation of the signal on the camera was made by reducing the exposure time, and a 1×1 mm ROI was arbitrarily chosen and kept the same for all shots. Using the chicane delay at $\Delta t = 0$ fs the electron beam was directly imaged on the diamond for both single-bunch and two-bunch mode as shown in Fig. 3. The two-bunch configuration is particularly relevant for the CBXFEL project which attempts to achieve a two-pass gain in the cavity. The two-bunch mode consists of the electron beam temporally separated into two bunches by ~ 218 ns delay which matches the recirculation time of the X-ray pulse across the cavity round trip. We demonstrated that Station F is capable of recording both bunches individually with the diamond target.

Furthermore, the results are also relevant to directly measure the position and size of the beam in single-bunch and two-bunch mode. Using the chosen ROI an image projection along the X and Y directions was calculated and plotted in Fig. 3. The resulting beam shape resembles a gaussian function rather closely, and thus the following function was fit to each of the projections: $f(x) = A * \exp(-(x - x_0)^2 / 2\sigma^2) + C$. In order to find the best fit parameters for A, x_0, σ and C .

Analyzing the gaussian fit obtained for every shot we observe an electron beam with two important features:

1. The position of the beam is relatively stable inside the ROI (doesn't jitter excessive amounts).
2. The size of the beam is in the order of a hundred microns.

Specifically, the mean width of the beam and the uncertainty in size was obtained by analyzing the value of standard deviation σ for every shot. Similarly, the center position of the gaussian x_0 was obtained for every shot to quantify the shot-to-shot jitter. Measured across multiple shots the size of the electron beam resulted in $\sigma_x = 94 \pm 22 \mu\text{m}$, $\sigma_y = 95 \pm 27 \mu\text{m}$ and its mean position on the diamond screen was $x_0 = 3 \pm 13 \mu\text{m}$, $y_0 = 15 \pm 7 \mu\text{m}$.

Notably, we observed that the electron beam size on the diamond target was decreased with increasing laser heater intensity. The observation is consistent with the expected suppression of microbunching instability at higher heater energies, which in turn leads to improved beam quality and reduction in beam size. While microbunching suppression reduced the emitted background radiation, this also makes the crystal more prone to saturation effects.

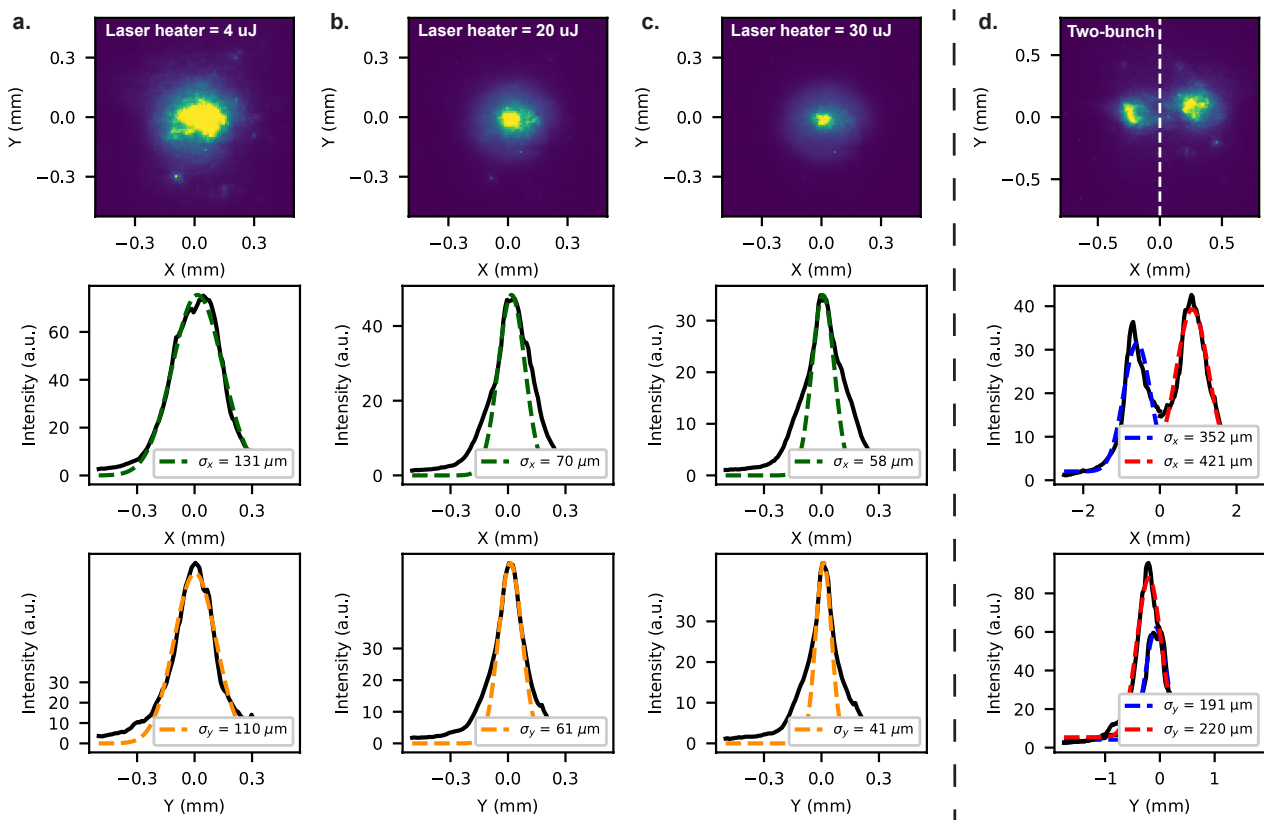


Figure 3: Direct observation of LCLS electron beam on diamond target for different operating modes and laser heater energy E . First, single-bunch mode with **a.** $E = 4 \mu\text{J}$, **b.** $E = 20 \mu\text{J}$, and **c.** $E = 30 \mu\text{J}$. As well as **d.** two-bunch mode.

DISCUSSION

One interesting aspect that was observed during this study is that the luminescence intensity and electron beam size changes more than expected from shot to shot. With some shots displaying a small faint beam while others a large bright beam, in some shots the beam is more distorted than others as well. These effect could be due to capturing different times during the luminescence process of the diamond and jitter in the electron beam parameters (charge, peak current, beam size). Detailed knowledge of the best time to image the target with respect to its luminescence lifetime has not yet been established. In the future a better trigger/timing calibration will need to be applied.

Furthermore, one of the biggest challenges in the study was encountered once the chicane delay was decreased to $\Delta t < 65 \text{ fs}$ and significant losses along the undulator line were observed resulting in faults from the Beam Loss Monitors (BLM). This effect can be understood as we consider that at a delay value of $\Delta t = 50 \text{ fs}$ in the chicane the displacement of the electron beam from its nominal trajectory at the Station F location is $\sim 2 \text{ mm}$. Taking into account the location where the deflected beam trajectory crosses the diamond at a location of $\sim 1.7 \text{ mm}$ from the edge, then at $\Delta t = 50 \text{ fs}$ the beam distance from the edge of the target would only be $\sim 300 \mu\text{m}$. At $300 \mu\text{m}$ from the edge the beam halo may already interact with the diamond, which could be the explanation for the BLM signals observed. Lastly,

for future studies it would be important to take the electron beam reference on the degaussed chicane, as opposed to the $\Delta t = 0 \text{ fs}$ delay setting.

CONCLUSION

In this study, we directly observed and measured the LCLS electron beam in single- and two-bunch modes. The electron beam position was observed to be relatively stable at $\pm 10 \mu\text{m}$ with a size of $\sim 100 \mu\text{m}$ on target. While we acknowledge uncertainties in the beam size measurement, the values seem close to the expected ones in this area, and the ability to measure the size and position during the two-bunch mode is particularly relevant for the CBXFEL project when attempting X-ray overlap with the second electron bunch. Finally, the ability of Station F to study microbunching effects in the accelerator is rather positive. This indicates that the BOD instrument can not only serve as a spatiotemporal diagnostic of the electron beam, but also aid in diagnosing beam quality parameters that otherwise would remain difficult to observe.

ACKNOWLEDGEMENTS

This work is supported by U.S. Department of Energy Contract No. DE-AC02-76SF00515. The authors thank A. Marinelli, Y. Ding, J. Cryan, C. Takacs, P. Liu, C. Curtis, G. Lanza (SLAC), Y. Shvydko (ANL) for insightful discussions and help with commissioning. We also thank the LCLS operations team.

REFERENCES

- [1] K-J Kim, Y. Shvyd'ko, and S. Reiche, "A proposal for an X-ray free-electron laser oscillator with an energy-recovery Linac", *Physical Review Letters*, vol. 100, no. 24, p. 244802, Jun. 2008. doi:10.1103/PhysRevLett.100.244802
- [2] Z. Huang and R. D. Ruth, "Fully coherent X-ray pulses from a regenerative-amplifier free-electron laser", *Physical Review Letters*, vol. 96, no. 14, p. 144801, Apr. 2006. doi:10.1103/PhysRevLett.96.144801
- [3] G. Marcus *et al.*, "Regenerative amplification for a hard X-ray free-electron laser", in *Proc. FEL'19*, Hamburg, Germany, Aug. 2019, pp. 118–121. doi:10.18429/JACoW-FEL2019-TUP032
- [4] W. Qin *et al.*, "Start-to-end simulations for an X-ray FEL oscillator at the LCLS-II and LCLS-II HE", in *Proc. FEL'17*, Santa Fe, NM, USA, Aug. 2017, pp. 247–250. doi:10.18429/JACoW-FEL2017-TUC05
- [5] E. Allaria and G. De Ninno, "A step towards cavity-based X-ray free electron lasers", *Nature Photonics*, vol. 17, no. 10, pp. 841–842, Oct. 2023. doi:10.1038/s41566-023-01302-0
- [6] P. Liu *et al.*, "X-ray diagnostics for the cavity-based x-ray free-electron laser project", *Physical Review Accelerators and Beams*, vol. 27, no. 11, p. 110701, 2024. doi:10.1103/PhysRevAccelBeams.27.110701
- [7] H. Kawarada, Y. Yokota, Y. Mori, K. Nishimura, and A. Hiraki, "Cathodoluminescence and electroluminescence of undoped and boron-doped diamond formed by plasma chemical vapor deposition", *Journal of Applied Physics*, vol. 67, no. 2, pp. 983–989, 1990. doi:10.1063/1.345708
- [8] L. Robins, E. Farabaugh, and A. Feldman, "Cathodoluminescence spectroscopy of free and bound excitons in chemical-vapor-deposited diamond", *Physical Review B*, vol. 48, no. 19, p. 14167, 1993. doi:10.1103/PhysRevB.48.14167
- [9] J. A. Freitas Jr., K. Doverspike, P. B. Klein, Y. L. Khong, and A. T. Collins, "Luminescence studies of nitrogen-and boron-doped diamond films", *Diamond and Related Materials*, vol. 3, no. 4–6, pp. 821–824, 1994. doi:10.1016/0925-9635(94)90277-1
- [10] D. Cesar *et al.*, "Ultrafast quantum dynamics driven by the strong space-charge field of a relativistic electron beam", *Optica*, vol. 10, no. 1, pp. 1–10, 2022. doi:10.1364/OPTICA.471773